In vivo application of electrical rejuvenation pulses to chronically implanted neural macroelectrodes in nonhuman primates for regulation of interface properties

O'Sullivan KP, Baker JL, Philip B, Orazem ME, Otto KJ and Butson CR

Abstract*- Chronically implanted neural electrodes have become an increasingly important tool in both research and clinical applications, where long-term viability and stability of the electrode-tissue interface (ETI) may be a critical factor in device performance. However, chronic implantation of electrodes in brain tissue typically results in distinct changes to the electrode-tissue interface (ETI), observed as a semicircular arc "tissue component" in Nyquist plots of electrochemical impedance spectroscopy (EIS) measurements. These alterations to electrode-tissue interface properties can interfere with electrode recording characteristics, increase stimulation thresholds, and may create unpredictable behavior in closed-loop applications where neural recordings are used as a control signal. Previous work[1,2] has demonstrated the potential for direct-current electrical rejuvenation to reduce the impact of "tissue component" impedance on measured EIS spectra in microelectrodes chronically implanted in rodents. Our aim here is to further investigate this phenomenon using macroelectrodes in nonhuman primates (NHPs). Scaled versions of human deep brain stimulation (DBS) and electrocorticography (ECoG) electrodes were chronically implanted in an adult male rhesus macaque nonhuman primate. Both direct-current and alternating-current electrical rejuvenation pulses were found to be sufficiently effective at reducing the appearance of "tissue component" in EIS measurements and dropping impedance, with further investigation needed to determine optimal parameters.

I. INTRODUCTION

Devices implanted in the brain typically elicit a foreign body response (FBR) under chronic conditions, involving the formation of scar tissue surrounding the implant. This tissue reaction can interfere with both recording and stimulation by reducing sensitivity to neural activity (Polikov *et al.*., 2005) and increasing stimulation thresholds necessary to elicit a desired response (Dhillon *et al.*., 2005, Rossini *et al.., 2010*). Such changes are characterized by the appearance of a semicircular capacitive "tissue component" in EIS data (Figure 1). These ETI changes may be of particular concern in closed-loop implant applications, where recordings from a chronically implanted electrode are used as a control signal to determine device behaviors such as the delivery of stimulation or drugs. In such devices, day-to-day deviations in ETI characteristics resulting from FBR development may result in erratic device performance or loss of reliability. It is therefore desirable to develop a means of regulating ETI properties to maintain predictable recording characteristics.

Previous work has demonstrated the potential for short-duration electrical pulses ("electrical rejuvenation") to reduce the influence of chronic tissue changes on the characteristics of an ETI (Otto *et al.*, 2006, Johnson *et al.*, 2004), particularly in microelectrodes chronically implanted in rodents. Electrical rejuvenation was shown to reduce the appearance of "tissue component" capacitive effects in electrochemical impedance spectroscopy (EIS) measurements, indicating a return of the ETI to a state resembling initial implant conditions before the development of chronic FBR. The object of our work was to further investigate this phenomenon in a more clinically applicable analogue, using scaled-down versions of clinical electrode types in a nonhuman primate (NHP) animal model. Both direct-current (DC) and alternating-current (AC) pulse types were applied, to investigate optimal rejuvenation pulse parameters. In addition, computational modeling

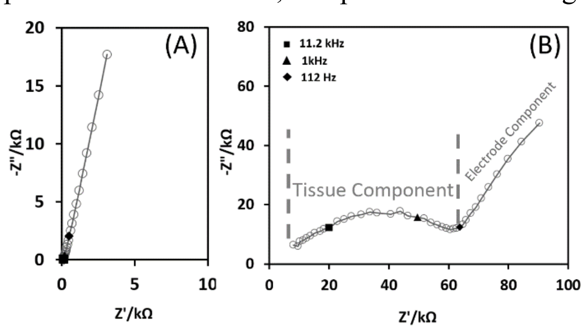

Figure 1- (A) An example Nyquist plot showing EIS data for an electrode immersed in phosphate-buffered saline (PBS). (B) Nyquist plot of an ECOG electrode chronically implanted in a nonhuman primate, showing a distinct capacitive "Tissue Component".

2023 11th International IEEE/EMBS Conference on Neural Engineering (NER) | 978-1-6654-6292-1/23/$31.00 ©2023 IEEE | DOI: 10.1109/NER52421.2023.10123750

was performed on EIS recordings to further investigate mechanisms of action.

II. METHODS

A. Instrumentation

EIS recordings were performed using a Palmsens4 Potentiostat instrument (PalmSens BV, Netherlands) in 2-electrode mode, using a titanium screw mounted in the animal's skullcap as a combined counter/reference electrode. PalmSens MUX-8 multiplexer instruments were used to automate multi-channel recordings. Electrical rejuvenation was applied using an STG4002 stimulus generator (Multi Channel Systems MCS GmbH).

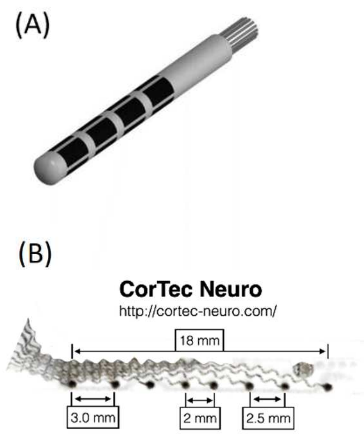

Figure 2- Macroelectrode types tested in this rejuvenation study. (A) Segmented Hereaus deep brain stimulation electrode. (B) 8 channel strip-style ECOG array (CorTec).

B. Rejuvenation

Direct-current (DC) and alternating current (AC) rejuvenation strategies were tested on 12-channel segmented DBS electrodes implanted in the animal's central thalamic nucleus (Hereaus Group, Hanau, Germany), as well as an epidural single-row (8 ch) strip (Fetz Spinal Cord 8, Cortec Neuro, Freiburg, Germany). Rejuvenation pulses were applied and included a 1 V DC pulse for a duration of 4 seconds per electrode contact, as well as AC strategies under voltage control at 1 V and current control at 1 mA spanning a range of frequencies (1 Hz-10 kHz). In-vivo electrical impedance spectroscopy was performed pre- and post- rejuvenation, measured between 10 Hz and 10 kHz. EIS measurements were repeated 3 times for each condition to facilitate experimental determination of the stochastic error structure. Model fitting and error structure analysis were performed using the Measurement Model software developed by Watson and Orazem (10.1149/osf.io/kze9x).

III. RESULTS

A. DBS electrode

Rejuvenation using identical protocols to those previously applied in a rodent microelectrode model (voltage-controlled rejuvenation at 1.5V DC, 4 seconds) (Otto *et al.*, 2006, Johnson *et al.*, 2004) produced favorable results in our DBS macroelectrode (Figure 3), achieving both the desired reduction in tissue component capacitance and an overall reduction in impedance magnitude across the frequency spectrum. Following these initial results, further rejuvenations were attempted using both DC and AC pulses. Subsequent rejuvenation attempts were performed using current-controlled stimulation at 1mA, as this was found to produce a longer-lasting effect. All pulses were applied for four seconds. Rejuvenation results for the DBS electrode are summarized in Figure 4, with impedance drops shown at 1 kHz.

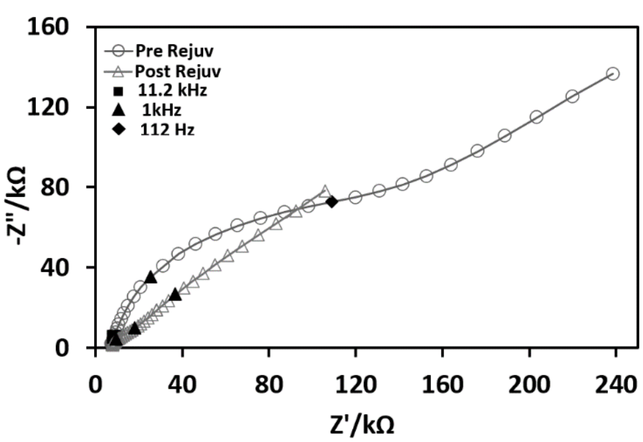

Figure 3-Nyquist plot showing EIS Spectra recorded before and after rejuvenation on one channel of a chronically implanted DBS electrode. Note the reduction in nonlinear "tissue component" characteristics as well as overall reduction in impedance magnitude following rejuvenation.

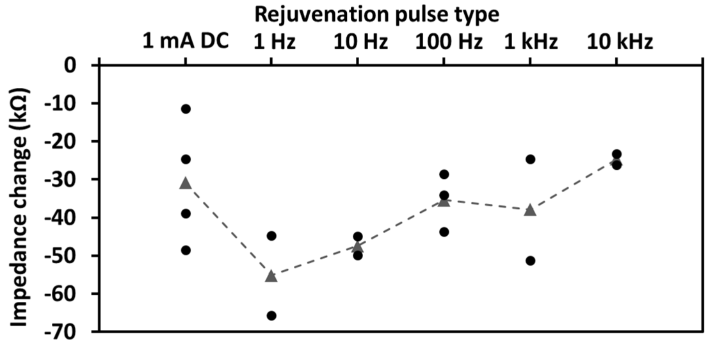

Figure 4- Rejuvenation results for a range of pulse types across channels of the segmented DBS lead. Black dots represent the difference in measured magnitude of 1 kHz complex impedance pre- and post- rejuvenation, with negative values denoting a drop in impedance. Each dot indicates one electrode contact rejuvenated at the frequency marked on the x-axis. Gray triangles indicate the average value within each grouping.

B. ECOG electrode

ECOG electrodes were rejuvenated with a similar protocol to the DBS electrode, using 1mA pulses for 4 seconds with both DC and AC configurations. In addition, EIS recordings were performed periodically post-rejuvenation for 7 days following initial stimulation to determine the longevity of effects. Nearly all current-controlled rejuvenation protocols were found to reduce impedance for approximately one week following initial stimulation (Figure 5), with 1kHz impedance values eventually returning to their pre-rejuvenation magnitude. A summary of rejuvenation results for the ECOG electrode is shown in Figure 6. With the exception of one channel, all protocol types were found to reduce impedance at 1kHz.

During our 3-week rejuvenation experiment, ECOG electrodes were measured periodically following initial stimulation to determine the window of efficacy of our impedance reduction. While previous experiments with voltage-controlled DC rejuvenation demonstrated a window of efficacy of around 24 hours (Otto *et al.*, 2006, Johnson *et al.*, 2004), we found that nearly all of our current-controlled AC rejuvenation protocols had effects lasting close to 7 days before original impedance values were recovered (Figure 6). This manifested as an initial reduction in the appearance of capacitive "tissue component" effects in EIS spectra, with the characteristic semicircular arc returning to EIS spectra with increasing size in subsequent measurements until reaching its original magnitude.

C. Model fitting

To verify good signal-to-noise ratio (SNR) and provide additional insights into our EIS measurements, model fitting and error structure analysis were performed using the Measurement Model software developed by Watson and Orazem (10.1149/osf.io/kze9x). The procedure followed a series of steps as outlined in Wang S *et al.* (2021). This began with regression of a Voigt measurement model

$$Z = R_{\mathrm{e}} + \sum_{\mathrm{k}=1}^{N} \frac{R_{\mathrm{k}}}{1 + j\omega\tau_{\mathrm{k}}} \quad (1)$$

which was used to fit each replicate spectrum for a given electrode and operating condition. The standard deviation of residual errors was used to estimate stochastic error. (Shulka *et al.*, 2004, Carson *et al.*, 2003).

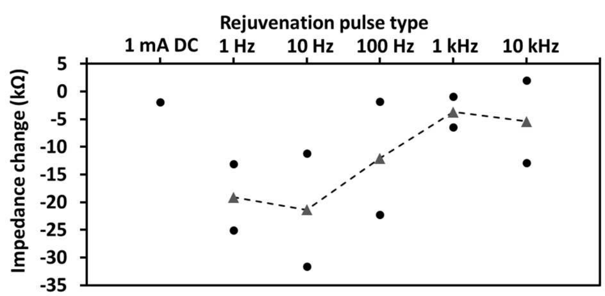

Figure 5- Rejuvenation results for the ECOG electrode. Dots represent the difference in magnitude of 1 kHz complex impedance pre- and post- rejuvenation. Gray triangles indicate the average value within each grouping. Note that all pulse types achieved some measure of impedance reduction with the exception of one channel at 10kHz, which had a slight increase (though it should be noted that impedance decreased at other frequencies for this measurement).

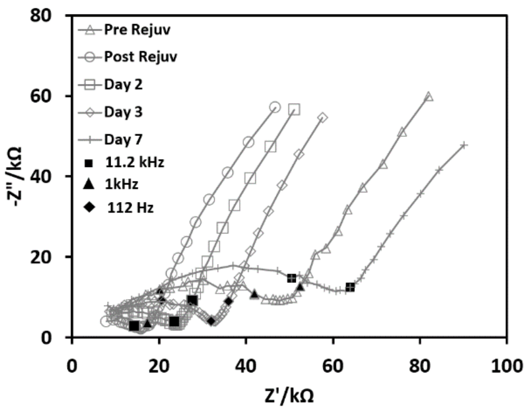

Figure 6-Nyquist plot of EIS results from a single ECOG channel, showing results before and after electrical rejuvenation, as well as the progression of its return to initial conditions over the course of 7 days. This channel was rejuvenated with a 10 kHz, 1mA pulse for 4 seconds.

This measurement model provided a means of filtering the bias errors that potentially confound replication of impedance spectra. An empirical model

$$\sigma = \sigma_{\mathrm{r}} = \sigma_{\mathrm{j}} = \alpha |Z_{\mathrm{j}}| + \beta |Z_{\mathrm{r}}| + \gamma |Z|^2 + \delta \quad (2)$$

was then fit to the standard deviations obtained by measurement model analysis, with regression weighted by stochastic error structure. Subsequent regressions were weighted by $1/\sigma^2$, where σ was obtained from equation (2).

Consistency of our impedance spectra with Kramers-Kronig relations was confirmed by fitting equation (1) to our measurements using either a weighted complex linear regression or regression to the real or imaginary part of impedance. The ability to provide a statistically satisfactory fit of the measurement model to an impedance spectrum demonstrates that the data satisfied the Kramers-Kronig relations (Figure 7). The analysis described above verified that our Palmsens4 Potentiostat provided data within an acceptable SNR.

IV. CONCLUSIONS

In compliance with results from previous rodent studies, our results demonstrate the efficacy of electrical rejuvenation as a strategy for regulating ETI properties in nonhuman primates. While most pulse types attempted achieved acceptable results, further investigation is needed to determine optimized rejuvenation parameters for practical applications in closed-loop neuromodulation systems.

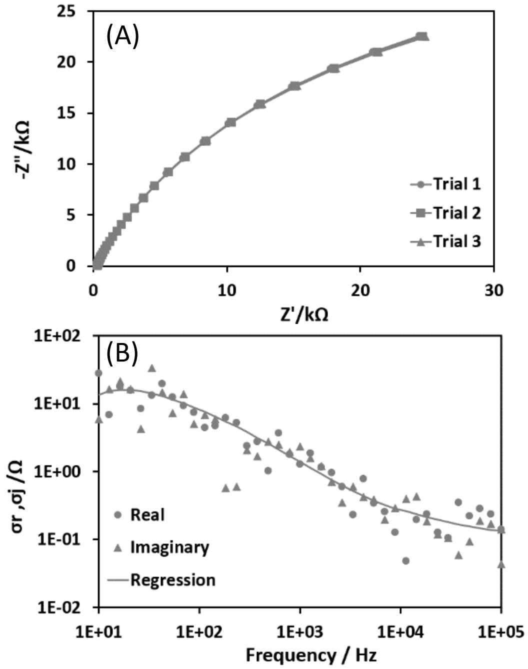

Figure 7- (A) Example of 3 repeated EIS measurements on an electrode channel. (B) Error regression model representing standard deviations of real and imaginary components of impedance. A good fit of the model indicates compliance with Kramers-Kronig relations and acceptable SNR.

V. REFERENCES

1. Otto KJ, Johnson MD, and Kipke DR (2006). Voltage pulses change neural interface properties and improve unit recordings with chronically implanted microelectrodes. *IEEE Transactions on Biomedical Engineering,* 53(2), 10.1109/TBME.2005.862530

2. Johnson MD, Otto KJ, Williams JC and Kipke DR (2004). Bias voltages at microelectrodes change neural interface properties in vivo. *IEEE Transactions on Biomedical Engineering*, DOI: 10.1109/IEMBS.2004.1404145

3. Polikov VS, Tresco PA and Reichert WM (2005). Response of brain tissue to chronically implanted neural electrodes. *Journal of Neuroscience Methods*, 148(1), pp. 1-28.

4. Dhillon GS, Kruger TB, Sandhu JS and Horch KW (2004). Effects of short-term training on sensory and motor function in severed nerves of long-term human amputees. *J. of Neurophysiology*, 93(5), pp. 2625-2633.

5. Rossini PM, Micera S, Benvenuto A, Carpaneto J, Cavallo G, Citi L, Cipriana C, Denaro L, Vincenzo D, Di Pino G, Ferreri F, Guglielmelli E, Hoffmann KP, Raspopovic S, Rigosa J, Rossini L, Tombini M and Dario P (2010). Double nerve intraneural interface implant on a human amputee for robotic hand control. *Clinical Neurophysiology*, 121(5), pp. 777-783.

6. Wang S, Zhang J, Gharbi O, Vivier V, Gao M and Orazem ME (2021). Electrochemical impedance spectroscopy. *Nature Reviews Methods Primers*, 1(41).

7. Shulka PK, Orazem ME and Crisalle OD (2004). Validation of the measurement model concept for error structure identification. *Electrochimica Acta*, 49(17-18), pp. 2881-2889.

8. Carson SL, Orazem ME, Crisalle OD and Garcia-Rubio L (2003). On the error structure of impedance measurements: Simulation of FRA instrumentation. *Journal of the Electrochemical Society*, DOI 10.1149/1.1605419